ANALYTICAL SCIENCES SEPTEMBER 2020, VOL. 36

Notes

Photolithographically Constructed Single ZnO Nanowire Device and Its Ultraviolet Photoresponse

Quanli Liu,[*1†] **Takao Yasui,**[*1,*2,*3†] **Kazuki Nagashima,**[*2,*4] **Takeshi Yanagida,**[*4,*5,*6] **Masafumi Horiuchi,**[*1] **Zetao Zhu,**[*1] **Hiromi Takahashi,**[*1] **Taisuke Shimada,**[*1] **Akihide Arima,**[*1] **and Yoshinobu Baba**[*1,*3,*7†]

*1 *Department of Biomolecular Engineering, Graduate School of Engineering, Nagoya University, Furo-cho, Chikusa, Nagoya 464–8603, Japan*
*2 *Japan Science and Technology Agency (JST), PRESTO, 4-1-8 Honcho, Kawaguchi, Saitama 332-0012, Japan*
*3 *Institute of Nano-Life-Systems, Institutes of Innovation for Future Society, Nagoya University, Furo-cho, Chikusa, Nagoya 464–8603, Japan*
*4 *Department of Applied Chemistry, Graduate School of Engineering, The University of Tokyo, 7-3-1 Hongo, Bunkyo, Tokyo 113–8656, Japan*
*5 *Institute of Scientific and Industrial Research, Osaka University, 8-1 Mihogaoka-cho, Ibaraki, Osaka 567–0047, Japan*
*6 *Institute of Materials Chemistry and Engineering, Kyushu University, 6-1 Kasuga-Koen, Kasuga, Fukuoka 816–8580, Japan*
*7 *Institute of Quantum Life Science, National Institutes for Quantum and Radiological Science and Technology, 4-9-1 Anagawa, Inage, Chiba 263–8555, Japan*

A sparse ZnO nanowire array with aspect ratio of *ca.* 120 and growth rate of 1 μm/h was synthesized by controlling the density of seeds at the initial stage of nanowire growth. The spatially-separated nanowires were cut off from the growth substrate without breaking, and thus were useful in the construction of a single-nanowire device by photolithography. The device exhibited a linear current–voltage characteristic associated with ohmic contact between ZnO nanowire and electrodes. The device further demonstrated a reliable photoresponse with an I_{UV}/I_{dark} of ~100 to ultraviolet light irradiation.

Keywords ZnO nanowire, single nanowire device, photolithography, ultraviolet photodetector

(Received January 17, 2020; Accepted April 7, 2020; Advance Publication Released Online by J-STAGE April 17, 2020)

Introduction

Single zinc oxide (ZnO) nanowire devices have been widely produced not only for use in research about intrinsic properties of ZnO at confined nanospace, but also for application in light-emitting diodes, photodetectors, and bio- and gas-sensors.[1-6] In general, the devices require high aspect ratio nanowires and use of costly electron beam (EB) lithography apparatuses, which present challenges for some researchers fabricating single nanowire devices.[7,8] For the first challenge, although metal–organic chemical vapor deposition (MOCVD) can yield high aspect ratio ZnO nanowires,[9,10] the severe experimental conditions, and high apparatus cost prevent it from being widely adopted. For less hazardous synthesis, flexible control by nutrient solution composition, and low cost, researchers generally select hydrothermal synthesis to produce ZnO nanowires.[11,12] In the hydrothermal synthesis, typical approaches to increase the aspect ratio of ZnO nanowires are, 1) adding polyethylenimine (PEI) to the growth solution to inhibit nanowire radial extension and prolong growth time,[13,14] or 2) adding $NH_3{\cdot}H_2O$ to promote nanowire axial growth and a PEI to inhibit radial extension.[15,16] For these two approaches, the former is bound by its slow growth rate, and the latter suffers from serious fusion at the bottom part of nanowires. For the second challenge of single nanowire device fabrication by transferring a single nanowire to a predefined location, single nanowire devices can be practically fabricated by photolithography,[17] but the complicated operation of picking up and transferring a single nanowire has to be implemented.

In the current work, we demonstrate a facile technique to hydrothermally synthesize a sparse ZnO nanowire array with high aspect ratio by suppressing the fusion at the bottom of nanowires. The fabricated nanowires were cut off from the growth substrate without breaking. A single-nanowire device was constructed *via* photolithography technique equipped with a micrometer control stage, instead of conventional EB lithography. Using the single-nanowire device, we characterized the electrical conduction properties of ZnO nanowires as well as their photoresponse to ultraviolet (UV) light irradiation.

† To whom correspondence should be addressed.
E-mail: liu.quanli@g.mbox.nagoya-u.ac.jp (Q. L.); yasui@chembio.nagoya-u.ac.jp (T. Y.); babaymtt@chembio.nagoya-u.ac.jp (Y. B.)

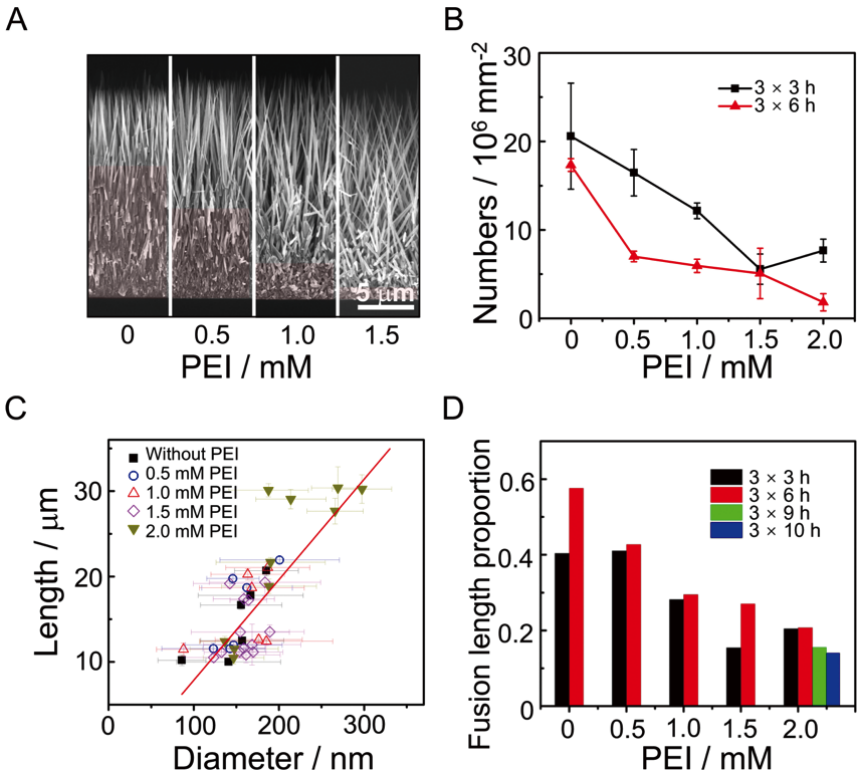

Fig. 1 Morphology analysis of ZnO nanowires. (A) SEM images of ZnO nanowires grown in nutrient solutions containing 800 mM ammonia and various weights of added PEI. (B) Numbers of nanowires in a unit area. (C) Nanowire diameter *vs.* its length for different weights of added PEI. The red line is a linear fit to the statistical data, and the error bars represent the standard deviation. (D) The proportion of bottom fusion length in the total length of the nanowires for different weights of added PEI.

Experimental

Growth and characterization of nanowires

Silicon substrates (N type) with a size of 20 × 10 × 0.625 mm were cleaned by heating them in a mixture of 98% concentrated sulfuric acid and 35% hydrogen peroxide (3:1 by volume) at 180°C for 2 h, and then washing them with ultrapure water and blowing them dry with a nitrogen gas flow. Radio frequency sputtering was used to prepare a 50-nm thick ZnO seed layer on the clean substrates. Next, the substrates were immersed into 50 mL nutrient solution in individual Teflon cups containing 50 mM equimolar of zinc nitrate hexahydrate and hexamethylenetetramine. Ammonia concentration was adjusted to 800 mM by adding 25% commercial ammonia solution. Then, 2 mM PEI (branched, low molecular weight, Aldrich) was added to the nutrient solution as a nanowire radial growth inhibitor, to result in a decreased nanowire areal density. The Teflon cups were covered with glass dishes and they were put into an oven, preheated to 95°C, and left for 3 h. After 3 h, the substrates were immersed into fresh solution in order to obtain long wire arrays; this was repeated 10 times (total immersion time of 30 h). In this way we were able to synthesize a 30-μm length nanowire array on each substrate in 30 h. Finally, the samples were washed with ultrapure water and acetone, before being dried on an 80°C hot plate for 10 min. We imaged the fabricated nanowires using a scanning electron microscope (SEM; Zeiss Supra 40 VP).

Device fabrication

The nanowires were cut from the substrates by a scalpel and suspended in isopropanol. The suspension was dropped onto a 20 × 20 mm SiO_2/Si substrate using a micropipette and dried in air. A layer of hexamethyldisilazane as tackifier was spin coated on the dried substrate with the nanowires at 3000 rpm for 8 s, and then this was covered with photoresist AZ 5200-E (purchased from Tokyo Ohka Kogyo) by spin coating at 1000 rpm for 120 s. Suitable nanowires were selected and they were exposed for the electrode pattern using photolithography equipment (Model DDB-700, Neoark Corporation). After pattern development, sputter-deposited electrodes were obtained that consisted of layers of Ti (10 nm), Pt (50 nm) and Au (100 nm).

Measurement of electrical resistivity

We measured resistance of the ZnO nanowires by the four probes measurement. A source meter (Model 2401, Keithly) was connected to two outer electrodes to provide the voltage and measure the current in circuit. A digital multimeter (34461A, Keysight) was connected to two inner electrodes and used for component voltage measurement. In photoresponse detection, the source meter was connected to two inner electrodes to provide a voltage and measure the current. A handheld UV lamp with wavelength of 365 nm (0.29 mW/cm^2) was used to illuminate the devices. The measurement was carried out in the dark in air.

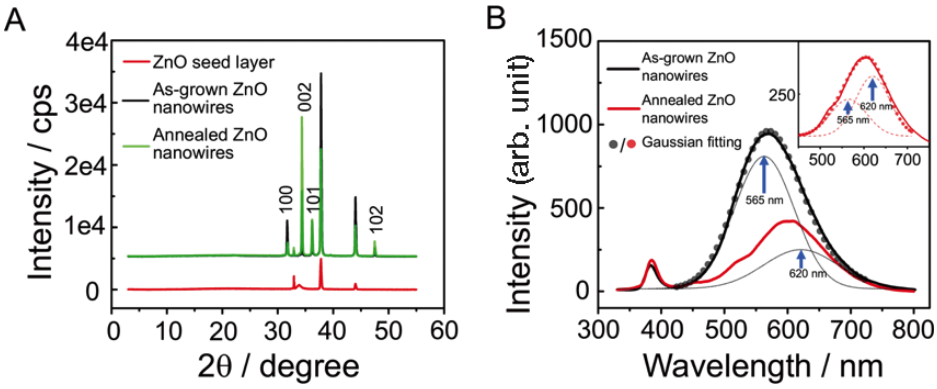

Fig. 2 Characterization of ZnO nanowires. (A) XRD patterns of ZnO nanowires and Si substrate with sputtered ZnO seed layer. Peaks with numbers on them indicate typical peaks for wurtzite characteristics. (B) Room temperature photoluminescence spectra of ZnO nanowires.

Results and Discussion

Research studies have shown that a certain amount of PEI hinders lateral growth of ZnO nanowires in solution.[13-16] In the current work, we carried out ammonia-assisted seed engineering with PEI as cation surfactant to control density of the seeds, realizing synthesized sparse nanowire arrays with ~120 aspect ratio at a 1 μm/h growth rate. According to the SEM images in Fig. 1A, it is clear that the areal density of the nanowires gradually decreases with the increased amount of added PEI. The statistical analysis in Fig. 1B confirms the inverse trend between nanowire areal density and the added PEI weight. This indicates that PEI plays a significant role on suppressing the initial nucleation. The statistical results in Fig. 1C demonstrate a small quantity of PEI has almost no effect on nanowire diameter and growth rate. We were able to boost the nanowire growth rate from 0.3 – 0.5 μm/h in typical experiments,[15,16] to 1 μm/h and produce an ultralong sparse ZnO nanowire array with ~120 aspect ratio. What is more, because of the low areal density, the serious fusion phenomenon of nanowires in the bottom part of the array is almost completely avoided (shades of light red in Fig. 1A). As shown in Fig. 1D, the fusion length proportion of total length gradually decreases with the increase of added PEI amount. The decrease of this proportion means that nanowires keep enough length for device fabrication after they are cut from the substrate.

According to XRD spectra of ZnO (JCPDS Card No. 36-1451), typical crystallographic peaks of ZnO nanowires (2 mM PEI, 27 h growth, ~30 μm length) are clearly seen in the XRD patterns (Fig. 2A). A significant increase of (002) peak intensity is measured after annealing nanowires at 600°C in vacuum for 2 h. The preferential nanowires growth orientation of [001] direction and improvement of crystallinity after annealing explain the prominent increase of (002) peak. The room temperature photoluminescence (PL) spectra and multiple Gaussian peak fitting (inset shows the fitting result of annealed ZnO nanowires) of green-yellow (~565 nm) and yellow-orange (~620 nm) defect emission in as-grown and annealed ZnO nanowires are shown in Fig. 2B. The dominant defect emission changes from green-yellow to yellow-orange after annealing, indicating the reduction and the reconstruction of ZnO crystal in nanowires. We consider the redshift of defect emission by decomposition of the possible presence of $Zn(OH)_2$ on the nanowire surface,[18] and the involvement of interstitial oxygen.[19] The bond breaking of the interstitial oxygen is supposed to weaken defect emission.[20] An intensity reduction and a redshift of the broad defect peak observed after heat treatment at 600°C in vacuum indicate a decrease in the point defect concentration and enhancement of crystallinity.

After obtaining ultralong nanowires, we employed a photolithography method to obtain single nanowire devices. The fabrication procedure is described in the experimental section and is as shown in Fig. 3A. Figure 3B intuitively presents nanowires cut from the substrate and deposited on a SiO_2/Si substrate using a micropipette, followed by drying it naturally in air. From the SEM image of the fabricated device shown in Fig. 3C, we can see that a four-terminal single nanowire device was neatly bridged between a 5-μm gap electrodes. Here, we carry out photolithography instead of electron beam irradiation to realize the structure of our single nanowire devices. The simpler procedures and less costly equipment will encourage more researchers to examine the electrical and optical properties of nanowires.

For a characterization of the nanowire electrical property, we measured electrical resistivity of the nanowire by the four probe sensing method (Fig. 4A). Figure 4B presents the I–V characteristics of the nanowires; we see that linear behaviors were achieved between [–0.25 V, +0.25 V]. The result demonstrates that good ohmic contacts between nanowires and metal electrodes have been realized. We estimated nanowire resistivities by Ohm's law based on the measurement of nanowire diameters and channel lengths between the inner two electrodes. Existence of the shallow energy level defects suggest that possibly the oxygen vacancy or the Zn interstitial defects result in an effective enhancement of electrical conductivity. The calculated resistivities vary in a range from 2.8 to 26.9 Ω·cm, which are comparable with previous studies.[21] To characterize the nanowire photoconductive properties, electrical measurements were performed in the states of UV light on and UV light off. Figure 4C compares the current–voltage (I–V) curves measured on a device with 5 μm length nanowire channel. Results show that, without UV illumination, the detected average resistance is above 15.1 MΩ and that indicates the nanowire is highly insulated in the dark; while when the device is exposed to UV light, the nanowire resistance is 1.9 MΩ, and that is a decrease by almost 1 order of magnitude. What is more, no matter with or without UV light irradiation, the current–voltage curves exhibit quite good linear behavior. The characteristics of the photoconductive ZnO nanowire

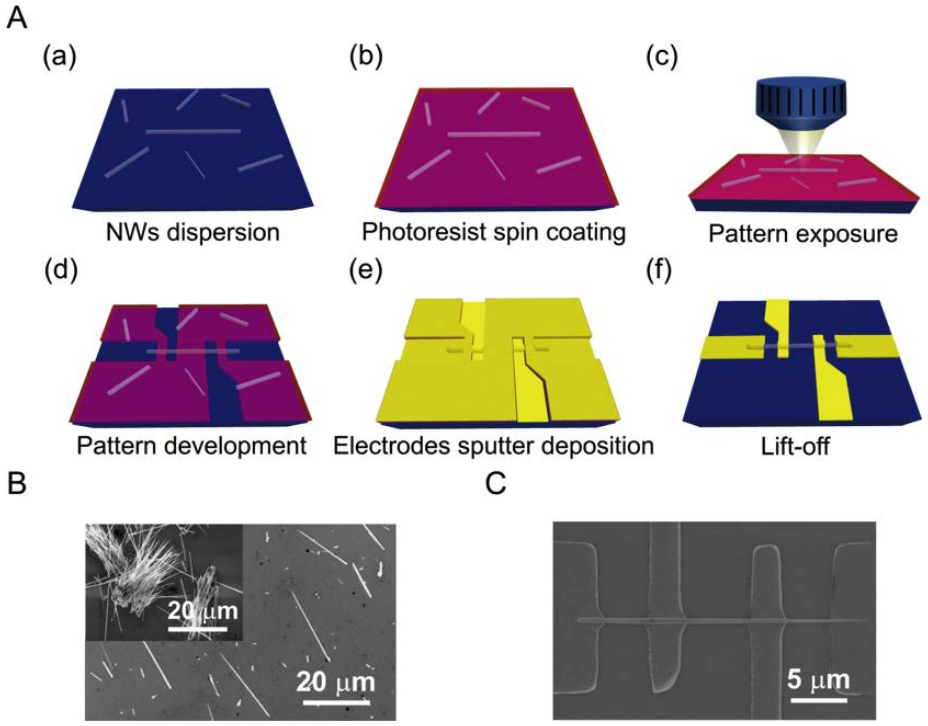

Fig. 3 Schematic drawings of the fabrication of the single nanowire device and SEM images of the device. (A) Schematic drawings of the fabrication. (a) Applying a suspension containing nanowires to a substrate followed by drying. (b) Covering with photoresist. (c) Selecting the suitable nanowires, and exposing the pattern. (d) Developing the pattern. (e) Sputter-depositing the metal electrodes. (f) Lifting-off excess photoresist and metal layer. (B) SEM image of ZnO nanowires cut from the substrate before (inset) and after 2 s ultrasonic dispersion. (C) SEM image of the single nanowire device. Distance between two adjacent electrodes was 5 μm.

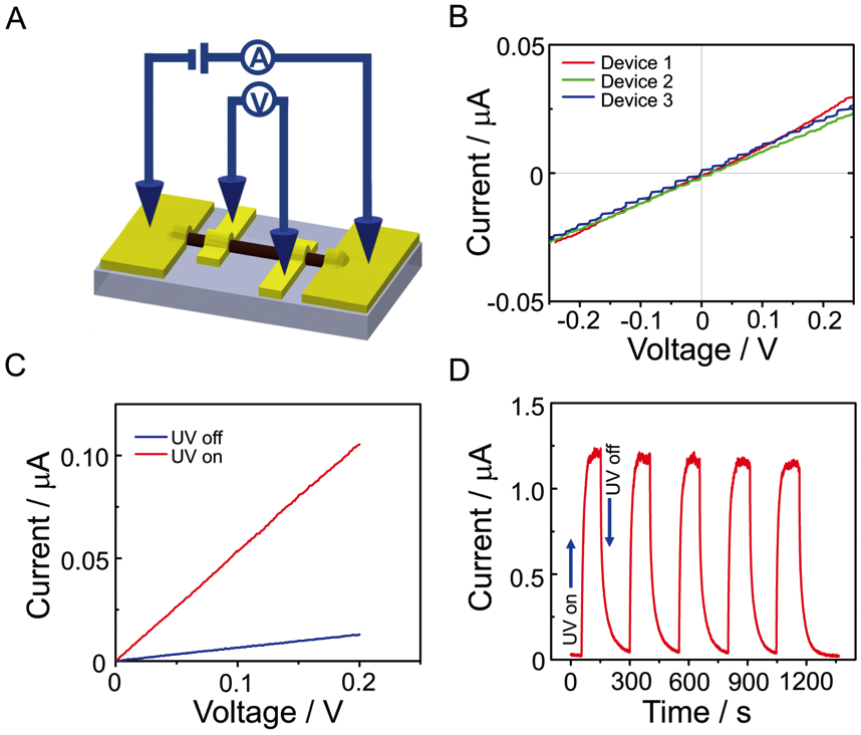

Fig. 4 Schematic of the four probe sensing method and device photoelectric properties. (A) Schematic of the four probe sensing method. Voltage between the two inner electrodes was measured by a digital multimeter. A source meter was used to apply the voltage and measure current. (B) Current–voltage (I–V) curves of several devices. (C) I–V curves of dark current (blue) and photocurrent (red) of a single ZnO nanowire device under UV illumination. (D) Device photo response to UV light being turned on and off, the bias on the nanowire is 1 V

suggest that it is a good candidate for a UV photodetector. Figure 4D shows the photoresponse to UV light being turned on and off as a function of time. Significant differences of the detected current clearly indicate that the fabricated UV detector can be reversibly switched between the low (dark) and the high (UV) conductivity states. With 1 V bias, our UV detector exhibits a ~100 (I_{UV}/I_{dark}) sensitivity, 23 s response time and 70 s recovery time. The photoconductive nanowire seems to be a good candidate for highly sensitive UV light detectors, and chemical or biological sensors when combined with suitable surface modification.

Conclusions

In summary, we successfully suppressed the fusion of nanowires at their bottom part and promoted nanowire growth rate to 1 μm/h by ammonia-assisted seed engineering and PEI as cation surfactant to control areal density of the seeds. With ~120 aspect ratio, nanowires were used to fabricate single-nanowire devices by a manageable photolithography apparatus. We estimated nanowire resistivities to be in the range of 2.8 to 26.9 Ω·cm due to ohmic contacts between the single nanowire and metal electrodes. The device exhibited a ~100 (I_{UV}/I_{dark}) sensitivity on exposure to UV irradiation, which enabled it to serve as UV light detector or switching device.

Acknowledgements

This research was supported by PRESTO (JPMJPR151B, JPMJPR19H9), Japan Science and Technology Agency (JST), the JSPS Grant-in-Aid for Young Scientists (A) 17H04803, the JSPS Grant-in-Aid for Scientific Research (A) 16H02091, the JSPS Grant-in-Aid for Scientific Research (S) 18H05243, a research grant from the Murata Science Foundation, Advanced Technology Institute Research Grants 2019, Foundation of Public Interest of Tatematsu, the Nitto Foundation, and the Nanotechnology Platform Program (Molecule and Material Synthesis) of the Ministry of Education, Culture, Sports, Science and Technology (MEXT).

References

1. D. Kalblein, H. Ryu, F. Ante, B. Fenk, K. Hahn, K. Kern, and H. Klauk, *ACS Nano*, **2014**, *8*, 6840.
2. J. Bao, M. A. Zimmler, and F. Capasso, *Nano Lett.*, **2006**, *6*, 1719.
3. L. Zhang, Y. Wang, H. Wu, M. Hou, J. Wang, L. Zhang, C. Liao, S. Liu, and Y. Wang, *Nanoscale*, **2019**, *11*, 8319.
4. E. Danielson, V. Dhamodharan, A. Porkovich, P. Kumar, N. Jian, Z. Ziadi, P. Grammatikopoulos, V. A. Sontakke, Y. Yokobayashi, and M. Sowwan, *Sci. Rep.*, **2019**, *9*, 17370.
5. A. Choi, K. Kim, H.-I Jung, and S. Y. Lee, *Sens. Actuators, B*, **2010**, *148*, 577.
6. Y. Hu, J. Zhou, P.-H. Yeh, Z. Li, T.-Y. Wei, and Z. L. Wang, *Adv. Mater.*, **2010**, *22*, 3327.
7. L. Oleg, C. Vasilii, P. Vasile, A. Mahdi, B. R. Beatriz, C. Lee, T. Ion, V. Bruno, P. Thierry, and A. Rainer, *Sens. Actuators, B*, **2016**, *223*, 893.
8. A. Choi, K. Kim, H. Jung, and S. Y. Lee, *Sens. Actuators, B*, **2010**, *148*, 577..
9. L. Hu, Q. Liao, Z. Xu, J. Yuan, Y. Ke, Y. Zhang, W. Zhang, G. P. Wang, S. Ruan, Y.-J. Zeng, and S.-T. Han, *ACS Photon.*, **2019**, *6*, 886.
10. T. Lim, J. Bong, E. M. Mills, S. Kim, and S. Ju, *ACS Appl. Mater. Interfaces*, **2015**, *7*, 16296.
11. J. Joo, B. Y. Chow, M. Prakash, E. S. Boyden, and J. M. Jacobson, *Nat. Mater.*, **2011**, *10*, 596.
12. S. Xu and Z. L. Wang, *Nano Res.*, **2011**, *4*, 1013.
13. J. Qiu, X. Li, F. Zhuge, X. Gan, X. Gao, W. He, S.-J. Park, H.-K. Kim, and Y.-H. Hwang, *Nanotechnology*, **2011**, *21*, 195602.
14. L.-Y. Chen, Y.-T. Yin, C.-H. Chen, and J.-W. Chiou, *J. Phys. Chem. C*, **2011**, *115*, 20913.
15. M. Law, L. E. Greene, J. C. Johnson, R. Saykally, and P. Yang, *Nat. Mater.*, **2005**, *4*, 455.
16. C. Xu, P. Shin, L. Cao, and D. Gao, *J. Phys. Chem. C*, **2010**, *114*, 125.
17. Q. Li, S.-M. Koo, C. A. Richter, M. D. Edelstein, J. E. Bonevich, J. J. Kopanski, J. S. Suehle, and E. M. Vogel, *IEEE Trans. Nanotechnol.*, **2007**, *6*, 256.
18. H. Zhou, H. Alves, D. M. Hofmann, W. Kriegseis, B. K. Meyer, G. Kaczmarczyk, and A. Hoffmann, *Appl. Phys. Lett.*, **2002**, *80*, 210.
19. F. Han, S. Yang, W. Jing, K. Jiang, Z. Jiang, H. Liu, and L. Li, *Opt. Express*, **2014**, *22*, 11437.
20. L. E. Greene, M. Law, J. Goldberger, F. Kim, J. C. Johnson, Y. Zhang, R. J. Saykally, and P. Yang, *Angew. Chem., Int. Ed.*, **2003**, *42*, 3031.
21. W. Geng, S. Kostcheev, C. Sartel, V. Sallet, M. Molinari, O. Simonetti, G. Lérondel, L. Giraudet, and C. Couteau, *Phys. Status Solidi C*, **2013**, *10*, 1292.